Anaerobic digestion at high-pH and alkalinity for biomethane production
Insights into methane yield, biomethane purity, and process performance

Diniz, Beatriz C.; Wilfert, Philipp; Sorokin, Dimitry Y.; van Loosdrecht, Mark C.M.

DOI
10.1016/j.biortech.2025.132505

Publication date
2025

Document Version
Final published version

Published in
Bioresource Technology

Bioresource Technology 429 (2025) 132505

Contents lists available at ScienceDirect

Bioresource Technology

journal homepage: www.elsevier.com/locate/biortech

Anaerobic digestion at high-pH and alkalinity for biomethane production: Insights into methane yield, biomethane purity, and process performance

Beatriz C. Diniz [a,*], Philipp Wilfert [a,b], Dimitry Y. Sorokin [a,c], Mark C.M. van Loosdrecht [a]

[a] Department of Biotechnology, Faculty of Applied Sciences, Delft University of Technology, Van der Maasweg 9, Delft 2629 HZ, the Netherlands
[b] Labor für Siedlungswasserwirtschaft und Abfalltechnik, Fachbereich Bauwesen, Technische Hochschule Lübeck 23562 Lübeck, Germany
[c] Winogradsky Institute of Microbiology, Federal Research Centre of Biotechnology, Russian Academy of Sciences, Moscow, Russia

HIGHLIGHTS

- Continuous reactor operation for biomethanation of waste sludge at pH 9.3.
- Transition from hydrolysis-limited to a methanogenesis-limited AD process at the highest OLR tested.
- No influence of ammonia toxicity observed (up to 14 mM tested).
- pH profile can be reasonably well predicted through a chemical model.
- pH influenced methanogenic community composition.

GRAPHICAL ABSTRACT

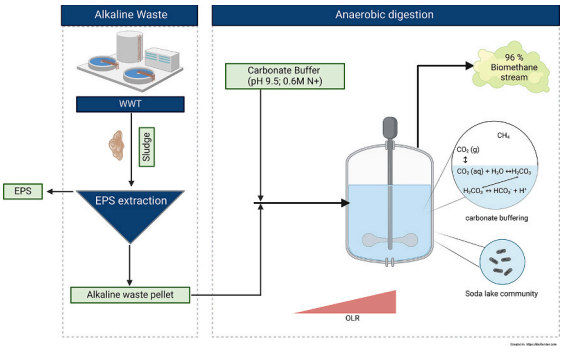

ARTICLE INFO

Keywords:
Anaerobic digestion
High-pH
High-alkalinity
Biogas upgrading
Methanocalculus
Alkaline waste

ABSTRACT

The role of high-pH conditions in anaerobic digestion (AD) has traditionally been confined to it's use in pretreatment processes. However, operating AD at elevated pH and alkalinity offers significant advantages, including in-situ upgrading of biogas to biomethane. This study examines the potential and scalability of AD under these conditions (pH ~ 9.3; alkalinity ~ 0.5 eq/L). The substrate used was the alkaline waste generated from the extraction of extracellular polymeric substances (EPS) from aerobic granular sludge (AGS), and the inoculum used was a haloalkaliphile microbial community from soda lake sediments. To evaluate the system's performance, the organic loading rate (OLR) was incrementally increased. The highest methane production obtained was 8.4 ± 0.1 mL/day/$g_{VSadded}$ at a hydraulic retention time (HRT) of 15 days and an OLR of 1 kg_{VS}/day/m^3. At this loading rate, methanogenesis became the rate limiting conversion. The maximum volatile solids conversion was 48.1 ± 1.1 %. Throughout the reactor operation, methane purity in the biogas consistently exceeded 90 % peaking at 96.0 ± 0.2 %, showcasing the potential for in-situ biogas purification under these conditions. In addition, no ammonia inhibition was observed, even with free-ammonia (NH_3) concentrations

Abbreviations: AD, anaerobic digestion; SBR, sequence batch reactor; HRT, hydraulic retention time; OLR, organic load rate; VS, Volatile solids; TS, total solids; COD, chemical oxygen demand; VFA, volatile fatty acids; TA, total alkalinity; CA, carbonate alkalinity; AGS, aerobic granular sludge; EPS, extracellular polymeric substances.

* Corresponding author at: Van der Maasweg 9, Delft 2629 HZ, the Netherlands.
E-mail address: M.B.canongialopescorreiadiniz@tudelft.nl (B.C. Diniz).

https://doi.org/10.1016/j.biortech.2025.132505
Received 24 January 2025; Received in revised form 21 March 2025; Accepted 7 April 2025
Available online 10 April 2025

reaching up to 14 mM. This study underscores the potential of high-pH anaerobic digestion as a sustainable method for both waste treatment and energy recovery.

1. Introduction

In recent years, anaerobic digestion (AD) has gained interest as a sustainable technology, as it reduces waste volumes and simultaneously converts this waste into renewable energy (Cai et al., 2016). Anaerobic digestion is a microbial decomposition process that converts complex organic matter into simpler molecules until the end products of CH_4 and CO_2, also known as biogas (Kleerebezem, 2014). This process can be divided into four sequential steps performed by different anaerobic microorganisms in a microbial community: hydrolysis, acidogenesis, acetogenesis, and methanogenesis (Gujer & Zehnder, 1983; Labatut & Pronto, 2018). The kinetics for such sequential reactions are controlled by the slowest step, within anaerobic digestion, this typically depends on the substrate. Polymer hydrolysis is often reported to be the limiting step when dealing with complex organic substrates, while methanogenesis is often reported to be the rate-limiting step when using soluble organic substrates (Ma et al., 2013).

To increase the biodegradability of complex substrates pre-treatments can be used. This facilitates the breakdown of complex polymers into simpler compounds. Pre-treatments can be divided into chemical (acid or base), physical (temperature, pressure), or biological (enzymatic) (Boarino et al., 2024; Karthikeyan et al., 2024; Romero-Güiza et al., 2017). Alkaline pre-treatment is one of the most frequently proposed methods, where the substrate is incubated with a strong base, such as NaOH, KOH, Na_2CO_3 or NH_3. The high pH leads to the partial chemical breakdown of the complex organic matter with a potential for faster microbial conversion (Kim et al., 2016). After this pre-treatment, the substrate is typically brought to a neutral pH, after which the anaerobic digestion is performed (Toutian et al., 2021). This neutralization step is necessary as classical AD systems have an optimal operational pH between 7 and 8 (Weiland, 2010). Until recently the use of high-pH conditions within AD has been limited to waste pre-treatment. However, operating the digestion at a higher pH can bring certain advantages to this system, especially in CO_2 capture and in the direct production of methane gas.

In classical AD systems, the biogas produced is commonly composed of methane (55–70 %), carbon dioxide (30–45 %), and other gases (0–5 %) (Lora Grando et al., 2017). To obtain a high-caloric gas that can be injected into the gas grid, CO_2 has to be removed and a high methane content (~95 %) needs to be reached. For this purpose, ex-situ purification steps are used, such as membrane separation, amine scrubbing, or water scrubbing (Awe et al., 2017; Chen et al., 2015; Lombardi & Francini, 2020). These methods often have high energy consumption and high operational cost and efforts are being made to optimize them (Khan et al., 2021). Alternatively, this purification could be done in-situ, where the biogas upgrading is integrated into the existing anaerobic digester. The external biogas upgrading step could be skipped entirely if anaerobic digestion was performed at a higher pH than the reported optimal (pH > 8.5) and higher alkalinity conditions. This approach is typically overlooked due to prevailing acceptance that the methanogenic community cannot thrive at higher pH, due to ammonia toxicity (Khan et al., 2021).

Alkalinity (in solution) can be defined as the excess of proton acceptors (bases) over proton donors (acids). Within this definition, all chemical species in solution are classified as either a proton donor or proton acceptor in relation to the zero level of protons for its respective acid-base system (Middelburg et al., 2020). To this end, the total alkalinity can be defined as a proton balance (1).

$$\begin{aligned} \textit{Total alkalinity}\left[\frac{eq}{L}\right] = {} & \left[HCO_3^-\right] + 2\left[CO_3^{-2}\right] + \left[OH^-\right] + \left[B(OH)_4^-\right] \\ & + \left[HPO_4^{-2}\right] + 2\left[PO_4^{-3}\right] + \left[H_3SiO_4^-\right] + 2\left[H_2SiO_4^{-2}\right] \\ & + \left[NH_3\right] + \left[HS^-\right] + 2\left[S^{-2}\right] - \left[H^+\right] - \left[HF\right] - \left[HSO_4^-\right] \\ & - \left[H_3PO_4\right] \end{aligned} \tag{1}$$

The total alkalinity can be simplified to carbonate alkalinity (2). For a simple CO_2-H_2O system, the dissolved CO_2 reacts with H_2O forming carbonic acid (H_2CO_3) which in turn can be deprotonated into bicarbonate (HCO_3^-) and carbonate (CO_3^{2-}) depending on the pH (Boyd, 2020).

$$\textit{Carbonate alkalinity}\left[\frac{eq}{L}\right] = \left[HCO_3^-\right] + 2\left[CO_3^{-2}\right] + \left[OH^-\right] - \left[H^+\right] \tag{2}$$

Therefore, in anaerobic digestion, where CO_2 is produced, a high-pH and high-alkalinity environment will lead to the CO_2 being speciated towards bicarbonate/carbonate and consequently remaining in the liquid, forming a methane-rich gas stream. An extra advantage of operating at these conditions is the potential increase of biodegradability of the substrate due to the high pH (Daelman et al., 2016).

Alkaline fermentation requires a microbial community that is capable of producing methane at the given conditions: high soluble carbonate alkalinity, high pH, and relatively high salt concentrations. These microorganisms can be found in soda lakes. Soda lakes are naturally occurring environments with high sodium carbonate alkalinity resulting in an extremely high and stable pH (9.5–11) (Schagerl & Renaut, 2016; Sorokin et al., 2014). Soda lakes can be classified according to their total salinity: moderately saline (35–50 g/L), high saline (50–250 g/L), and hyper-saline (250 g/L-saturation). The level of salinity has a great impact on the functional microbial diversity (Oren, 1999; Sorokin et al., 2014).

The concept of anaerobic digestion at high-pH and high-alkalinity was first explored by Nolla-Ardèvol et al., (2015). Anaerobic digestion was performed at pH 10 and 2 M total Na^+ using microalga *Spirulina* biomass as substrate and soda lake sediments as an inoculum in a sequence batch reactor (SBR) regime. They obtained, a continuous biogas stream reaching a maximum concentration in methane of 86 ± 5 % but only a 11 % substrate conversion. The maximum methane production was 4.8 ± 1.0 mL CH_4/day/$g_{spir.added}$. The main bottleneck was hypothesized to be inhibition by free-ammonia (NH_3). As a higher pH leads to speciation towards free-ammonia (NH_3). The choice of substrate could have aggravated this inhibition, the low C/N ratio of the protein-rich cyanobacterial biomass results in significant ammonium generation (Gonzalez-Fernandez et al., 2015). To overcome this low substrate C/N ratio, Rincón-Pérez et al., (2021) co-digested hydrolysed microalgal biomass with cheese whey, a carbon-rich substrate. This digestion was done at a pH of 9 achieving a maximum methane production of 3.9 ± 1.5 mL CH_4/day/$g_{VSadded}$[1] and a maximum biogas CH_4 concentration of 89.8 ± 5 %. Their work was not done at high alkalinity conditions resulting in a low buffering capacity and a fast pH decrease in the batch digestion. Hence, the experimental conditions do not reflect the conditions that would occur in a stable continuous buffered anaerobic digester for biomethane production.

The current study tested high-pH AD on an alkaline waste stream. Alkaline waste streams are ideal substrates as it is possible to incorporate their inherent alkaline properties in this technology. The alkaline waste stream used in this work was generated from the extraction of extracellular polymeric substances (EPS) from aerobic granular sludge (AGS)

[1] This calculation was done including the VS concentration of the inoculum.

(Bahgat et al., 2023). This work aims to showcase the industrial potential of direct biomethanation at high-pH and high-alkalinity conditions using an alkaline organic-rich waste as a substrate in a continuous operated sequencing batch reactor. It represents a proof-of concept study of this technology and shows the effects of increasing the organic load rate (OLR) towards industrial competitive ranges. To address this, a sequence batch reactor fed with this wastewater sludge residue was operated at increasing organic load rates (OLR) and decreasing hydraulic retention times (HRT). The study started with a low OLR (0.4 $kg_{VS}/day/m^3$) and focused on small stepwise increases due to unestablished kinetics of the inoculum used and concerns over ammonia toxicity. This operation was accompanied by detailed analyses (VFA, NH_4, alkalinity, COD, gas production and purity, and mass balances) to understand the biomethane production process and identify potential bottlenecks, e.g., related to hydrolytic rates, pH variation, and ammonia toxicity. Based on the collected data a geochemical model was constructed to predict the pH behaviour and its relation to the biogas purity. Additionally, throughout the experimental period, the microbial community was monitored to identify its adaptation and dynamics.

2. Materials and methods

2.1. Medium, substrate preparation and inoculum

The alkaline waste was obtained from the demo extracellular polymeric substances (EPS) extraction installation at the municipal waste water treatment plant (WWT) in Epe, Netherlands (Bahgat et al., 2023). This extraction was performed to aerobic granular sludge (AGS). Characteristics of this alkaline waste are described in Table 1. and the method of extraction is described in (Bahgat et al., 2023).

This alkaline sludge residue was diluted in a carbonate buffered medium (Na+:0.6 M; pH 9.5) before being fed into the bioreactor in order to reach a specific VS concentration (Table 2).The buffered medium had the following composition: $NaHCO_3$ 20 g/L; Na_2CO_3 15 g/L; NaCl 3 g/L; K_2HPO_4 1 g/L and $MgCl{\cdot}6H_2O$ 0.2 g/L. To this buffered medium 0.1 mL of a selenium solution was added. The selenium solution had the following composition: $NaSeO_3$ 0.02 g/L; Na_2WO_4 0.03 g/L. Additionally, 1 mL of the acid trace metal solution described in (Pfennig & Lippert, 1966) was added. It is important to note, that this acid trace metal solution was modified by removing H_3BO_3 and by substituting $MnCL_2$ for $MnSO_4$.The original inoculum was retrieved from anoxic sediments of hypersaline soda lakes in Kundula steppe (Altai Region, Russia).It consisted of a mixture of sulfidic sediments (depth 5–20 cm) from five soda lakes. The total salt concentration was between 50 and 250 g/L, the pH between 9.8 and 11.0, and total carbonate alkalinity between 0.5 to 4 M (Vavourakis et al., 2018).

2.2. Sequence batch reactor operation

A sequence batch reactor with a 1 L liquid volume and 0.2 L headspace volume was used. To this reactor an influent and effluent vessel were connected. To maintain the 1L liquid volume constant, the same amount was fed and discharged every 12 h. The volume that was fed/discharged within this 12 h cycle was adjusted to reach a specific hydraulic retention time (HRT). The reactor was continuously mixed at a 150 RPM speed and maintained at a temperature of 35 °C through a thermostatic water bath. Additionally, the reactor was connected to an overpressure valve of 1.3 bar that controlled the maximum pressure in the reactor, this pressure was intermediately released for the measurement of the gas production (section 2.3). In this operation the HRT and sludge retention time (SRT) were coupled. The bioreactor was controlled with an in-control process controller (*Applikon*) and the pH was continuously measured through a pH probe. No external pH control was used in this system, the only pH control used was the carbonate buffer described in the section 2.1. Both influent and effluent vessels were flushed with argon to prior use, and an argon gas bag was attached to the influent bottle to replace the volume each time the reactor was fed.

Table 1
Composition of the alkaline sludge residue from EPS extraction of AGS from the WWT plant in Epe, NL. This residue was used as substrate in this work.

Solids (g/L)	Total solids (TS)	86.8 ± 0.3
	Volatile solids (VS)	64.8 ± 0.3
Elemental analysis (%)	C	34.1
	H	4.9
	N	2.9
	O	26.8
	C/N	11.7

Table 2
Operational information at different organic load rate phases of semi-batch reactor. For the operational volume of 1L, where HRT and SRT are coupled.

OLR ($kg_{VS}/day/m^3$)	0.4	0.5	0.6	0.8	1
Influent VS (g/L)	9.9 ± 0.5	13.5 ± 0.1	14.4 ± 0.3	15.9 ± 0.1	14.6 ± 0.8
Influent tCOD (g/L)	12.1	17.9	18.1	21.4	18.9
HRT (days)	25	25	25	19	15
Phase length (days)	39	87	55	38	27

For acclimatization purposes the sequence batch reactor was initially operated after inoculation at an organic load rate (OLR) of 0.4 $kg_{VS}/day/m^3$ and an HRT of 25 days for 8 consequently HRT cycles (200 days). After acclimatization, the reactor was operated at 5 different stages according to their OLR of 0.4, 0.5, 0.6, 0.8, and 1 $kg_{VS}/day/m^3$. The increase in OLR was done in the first three phases by increasing the influent VS concentration with a 0.1 $kg_{VS}/day/m^3$ increase and for the last two phases by decreasing the HRT at constant VS in the influent with a 0.2 $kg_{VS}/day/m^3$ increase (Table 2). After a full HRT cycle, each phase was further ran until a stable VS concentration in the effluent was reached and the mass balances closed according to the product reaction described in section 2.4. On average, this was achieved after 2 HRT cycles in each phase (Table 2).

2.3. Analytical methods

The gas production was measured via a pressure meter (*Cole Parmer 4–20 mA*) and the gas composition was measured, after collecting it in a gas bag, via the Prima-BT mass spectrometer (*Thermofisher*). The composition for CH_4, CO_2 was measured for all OLR stages, whilst H_2 composition was only possible to measure in the last two OLR stages, this composition remained below 0.15 %. Volatile solids (VS) and total solids (TS) were measured according to (APHA, 2017). Chemical oxygen demand (COD) was measured with the LCK114 test kit (*Hach Lange*). N-NH_4 and P-PO_4 were measured through a photometric analysis via the gallery discrete analyser (*Thermofisher*). Total alkalinity (TA) was measured through the standard titration method (Dunnivant, 2004). The elemental composition was determined by an elemental analyser (*Mettler Toledo*). The final results for TS, VS, COD, N-NH_4, and P-PO_4 represent an average of 3 distinct batch days within the same OLR stage. The measurements for each single batch day were measured in duplicate for N-NH_4, and P-PO_4 and in triplicate for TS and VS. All data was measured after a full HRT cycle for each OLR stage. The pH and pressure measurements represent an average of 6 distinct batch days within the same OLR stage.

Throughout the current work, methane is presented through different approaches to allow comparison with literature and to take into account substrate specificity. Firstly, methane is presented as a specific methane production rate ($mL/day/g_{VSadded}$) this refers to the production of methane through time (within an HRT cycle) normalized

to the VS of the influent. Secondly, methane is also presented as methane production rate (mL/L/day) this refers to the methane produced through time (within an HRT cycle) normalized to the reactor volume – 1L. Finally, methane is also presented as methane yield (mL/$g_{VSadded}$) this refers to the total methane produced within an HRT cycle normalized to the VS of the influent.

2.4. Theoretical specific methane production rate

In order to calculate the theoretical specific methane production rate a product reaction for the process was derived (equation (3)). The substrate formula was calculated according to the elemental analysis shown in Table 1, which was further normalized to carbon (C). Additionally, it was assumed that the final products for the substrate conversion were and CH_4, CO_2, NH_4HCO_3, H_2O.

$$CH_{0.09}O_{0.79}N_{0.14} \rightarrow 0.4CH_4 + 0.6CO_2 + 0.1NH_4HCO_3 - 0.8H_2O \quad (3)$$

Through equation (3), is possible to derive the theoretical potential for this process through the stoichiometry for CH_4 – 1 mol of substrate will lead to 0.4 mol of methane. Assuming, 1 g in substrate ($CH_{0.09}O_{0.79}N_{0.14}$) is equivalent to 1 g in VS, it is possible to convert the theoretical potential to 307 $mL_{CH4}/g_{VSconverted}$. This term, can be further used to calculate the theoretical specific methane production rate by using the VS difference between influent and effluent (ΔVS):

$$Theoretical\ specific\ CH4\ production\ rate\left[\frac{ml}{g_{VSadded}\cdot day}\right] = \frac{\Delta VS\cdot 307}{VS_{influent}\cdot HRT} \quad (4)$$

2.5. 16s Amplicon sequencing analysis

The sequence batch reactor was sampled throughout operation. 2 mL were sampled at the beginning of an HRT cycle (initial), usually at the mid-point of an HRT cycle and at the end of an HRT cycle. The latter, on average after stabilization phase of 2 complete HRT cycles (final). The DNA was extracted according to the DNAeasy UltraClean microbial kit protocol (*QIAGEN*). Amplicon generation, library preparation, and sequencing were further analysed by Novagene.

The total genome DNA, from the samples, was further extracted using the CTAB method, and the DNA concentration and purity were monitored on 1 % agarose gels. According to this concentration, DNA was diluted at 1 ng/L. The V4 and V3 regions of the microbial 16S ribosomal RNA gene were amplified by PCR. The PCR reactions were performed by 15 μL High-fidelity PCR master mix (*Phusion*), where 2 μM of forward and reverse V3-V4 rRNA primers were added and 10 ng of template DNA. The PCR products were identified by 2 % agarose gel and purified with the gel extraction kit (*QIAGEN*). Sequencing libraries were then generated by using TruSeq DNA PCR-Free preparation kit (*Illumina*). The library was sequenced on an Novaseq platform (*Illumina*) and 250 bp paired end reads were generated. The paired-end reads were then assigned to samples based on their respective barcode and truncated by cutting off the barcode and primer sequence.

Using the dada2 pipeline (Callahan et al., 2016) the paired-end sequences were merged and filtered for quality to obtain high-quality clean tags (Bokulich et al., 2013). After quality filtration, the sequences were clustered into the respective ASVs after the removal of the chimeric sequences. For each representative sequence, the SILVA 138.1 database was used to annotate the taxonomy information (Robeson et al., 2020). After annotating the taxonomy data was further processed in R software with the *phyloseq* package (McMurdie, 2017) for data visualization proposes. The raw sequences for each sample were submitted to the European Nucleotide Archive (ENA) under the accession number PRJEB83037.

2.6. PHREEQC analysis

To understand the pH behavior within the system a chemical model was established in geochemical model software PHREEQC v3.7.3. The database used was the *Amm.dat* database provided by the software. Initially, an input solution was created with the buffer concentrations described in section 2.1 at 35 °C and a pH of 9.3. This solution was then equilibrated with a fixed headspace volume (reactor headspace volume + volume of gas collection bag), where CH_4, CO_2, H_2O, and NH_3, were given as potential gases. The charge balance in the equilibration step was done with pH.

To the equilibrated solution, a reaction step was introduced. This step instructed a stepwise addition of CH_4, CO_2, H_2, and NH_3 to the solution within a 0–100 mM range. CH_4, CO_2, and NH_4 were added according to the stoichiometry of the product reaction in this 0–100 mM range (equation (3)). For each stepwise addition, an equilibrium solution was calculated, where the charge balance was done with pH. To each equilibrium point the pH and CH_4, CO_2, H_2, and NH_3 compositions were registered and plotted. The PHREEQC script can be found in the supplementary material. For comparison, this model was plotted together with experimental data for each OLR phase studied (Table 2) and additional experimental data point from the acclimatization phase (section 2.2) was also used.

3. Results

3.1. Overall reactor operation

Anaerobic digestion was performed to the alkaline sludge residue of extracellular polymer extraction from aerobic granular sludge (AGS) (Bahgat et al., 2023). This sludge was suspended in a carbonate buffer resulting in a influent with an original pH of ~ 9.3 and an alkalinity of ~ 0.5 eq/L (Table 3). The digestion was done in a sequencing batch reactor regime at different OLRs (0.4; 0.5; 0.6; 0.8 and 1 $kg_{VS}/day/m^3$). The OLR was first changed by increasing the initial volatile solid (VS) concentration of the influent (9.9; 13.5; 14.4 g/L) while the HRT was constant (25 days), thereafter the OLR was increased by decreasing the HRT (25;19;15 days). In Table 3, the results for each OLR stage are shown.

The general reactor operation is summarised in Table 3, where the experimental and theoretical specific methane production (mL/day/$g_{VSadded}$) according to the VS converted are shown. The overall methane production (ml/L/day) rate can be seen in Fig. 1. The theoretical calculations can be found in section 2.4. The theoretical and experimental specific methane production rates fall within the same standard deviation range for all OLR studied (Table 3). The difference between the averaged results remains below 15 % for all stages. For the OLRs of 0.6 and 1 $kg_{VS}/day/m^3$, the average specific experimental rate (6.2 ± 0.1 and 8.4 ± 0.1 mL/day/$g_{VSadded}$) was higher than the specific theoretical rate (5.9 ± 0.2 and 7.9 ± 1 mL/day/$g_{VSadded}$, respectively). This discrepancy is likely attributed to error propagation in the experimental measurements, and both values still fall within the same error range, demonstrating the validity of the calculations. Therefore, the methane production can be directly correlated with the degree of VS degradation. The VS conversion increased from 41 %, at the lowest OLR of 0.4 $kg_{VS}/day/m^3$, to 48 ± 0.7 % conversion at the OLR of 0.6 $kg_{VS}/day/m^3$. This conversion remained relatively constant until the last OLR of 1 $kg_{VS}/day/m^3$ where it decreased to 38 ± 1 %. This decrease in conversion is also reflected in the detection of acetate in the effluent, pointing to incomplete VS degradation. Acetate was only measured in the highest OLR (1 kg_{VS}/day/m3) at a concentration of 0.20 ± 0.05 mM, for the other OLRs the concentration was below the detection limit. This suggests that for the initial stages, acetate was fully converted into CH_4.

Table 3
Characteristics of influent, effluent and biogas streams in a sequence-batch reactor as function of the applied OLR ($kg_{VS}/day/m^3$). The digestion was performed with alkaline wastewater sludge residue generated during EPS extraction of AGS.

stream	OLR ($kg_{VS}/day/m^3$)	0.4	0.5	0.6	0.8	1
Influent	HRT	25	24	25	19	15
	Influent pH	9.27	9.35	9.27	9.37	9.44
	TS (g/L)	40.1 ± 0.4	43.1 ± 1.4	43.6 ± 0.4	43.9 ± 0.5	43.2 ± 0.3
	VS (g/L)	9.9 ± 0.5	13.5 ± 0.1	14.4 ± 0.3	15.9 ± 0.1	14.6 ± 0.8
	Total ammonia (mM)	12.0 ± 0.2	13.1 ± 0.2	20.2 ± 0.2	27.1 ± 0.3	25.2 ± 0.2
	PO_4 (mM)	10.9 ± 0.8	9 ± 0.7	10.1 ± 0.2	10.1 ± 0.3	10.4 ± 0.7
	Acetate (mM)	6.3 ± 1	9.7 ± 0.2	14.3 ± 0.5	8.8 ± 0.1	9.4 ± 0.1
	Total alkalinity (eq/L)	0.50	0.46	0.44	0.47	0.45
effluent	Operational pH	8.68 ± 0.01	8.60 ± 0.01	8.56 ± 0.03	8.61 ± 0.02	8.76 ± 0.01
	TS (g/L)	36.9 ± 2.1	40.8 ± 7.0	35.7 ± 0.9	36.4 ± 0.6	36.6 ± 1.1
	VS (g/L)	5.9 ± 0.3	7.2 ± 0.3	7.5 ± 0.4	8.6 ± 0.2	9 ± 0.6
	VS conversion (%)	40.9 ± 3.1	46.8 ± 1.7	48.1 ± 1.1	46.0 ± 1.2	38.3 ± 3.4
	Total ammonia (mM)	35.8 ± 2.3	38.0 ± 1.1	45.2 ± 0.6	50.0 ± 1.2	54.4 ± 0.6
	PO_4 (mM)	12.0 ± 0.2	11.8 ± 0.1	11.5 ± 0.1	11.1 ± 0.1	9.6 ± 1.1
	Acetate (mM)	na	na	na	na	0.20 ± 0.05
	Total alkalinity (eq/L)	0.51	0.52	0.50	0.57	0.47
Biogas	CH_4 (%)	96.0 ± 0.2	94.2 ± 0.2	92.5 ± 0.3	95.2 ± 0.1	95.8 ± 0.1
	CO_2 (%)	4.0 ± 0.1	5.8 ± 0.1	6.9 ± 0.1	4.8 ± 0.1	4.2 ± 0.1
	CH4 yield (mL/ $g_{VSadded}$)	113 ± 2	124 ± 3	151 ± 2	131 ± 6	125 ± 1
	Specific CH_4 production rate (mL/day/$g_{VSadded}$)	4.6 ± 0.1	5 ± 0.2	6.2 ± 0.1	6.9 ± 0.3	8.4 ± 0.1
	Theoretical specific CH_4 production rate [b] (mL/day/$g_{VSadded}$)	5.03 ± 0.6	5.7 ± 0.3	5.9 ± 0.2	7.4 ± 0.2	7.9 ± 1

[b] Calculated through the assumption that all volatile solids (VS) conversion was a result of CH_4 production according to the product reaction developed in section 2.4.

3.2. Methane production rate and purity

The increase in OLR both affected the methane production rate (mL/L/day) and the methane purity (%). With the increase in OLR, an increase in the methane production rate was observed, reaching a maximum of 122.4 ± 7 mL/L/day (Fig. 1 – right). Additionally, as expected, a biogas stream with high methane content (>90 % CH_4) was produced throughout the study, reaching a maximum of 96 ± 0.2 % (Fig. 1 – right).

The methane production rate increased linearly between OLRs 0.4–0.6 $kg_{VS}/day/m^3$, concomitantly there was a small, linear decrease in biomethane purity (Fig. 1). The methane production rate increased on average 30 % per 0.1 $kg_{VS}/day/m^3$ and methane purity decreased on average 1.8 % per 0.1 $kg_{VS}/day/m^3$. For the OLRs 0.8 and 1 $kg_{VS}/day/m^3$, with respective HRTs of 19 and 15 days, an increase in the methane production rate was observed, however at a slower pace. The methane production rate increased on average 10 % per 0.1 kg_{VS}/day. Additionally, for the OLRs 0.8 and 1 $kg_{VS}/day/m^3$ methane purity first increased by 3 % and then stabilized. The pattern between the CH_4 content in the gas phase and OLR was also mirrored in the relationship between the operational pH and the OLR (Fig. 2).

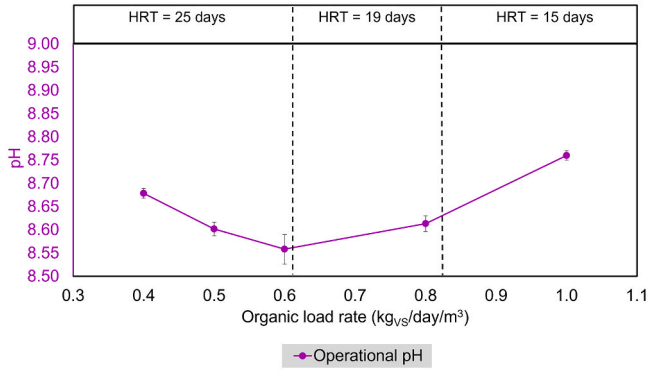

Fig. 2. Operational pH in the sequence batch reactor of the digestion of alkaline waste as function of the OLR studied ($kg_{VS}/day/m^3$; x-axis).

3.3. pH stability and its impact on gas composition

In this work, no external pH control was used, the system fully relied on the carbonate buffer in the influent (section 2.1). As a result, the reactor pH (operational pH) fluctuated slightly throughout the

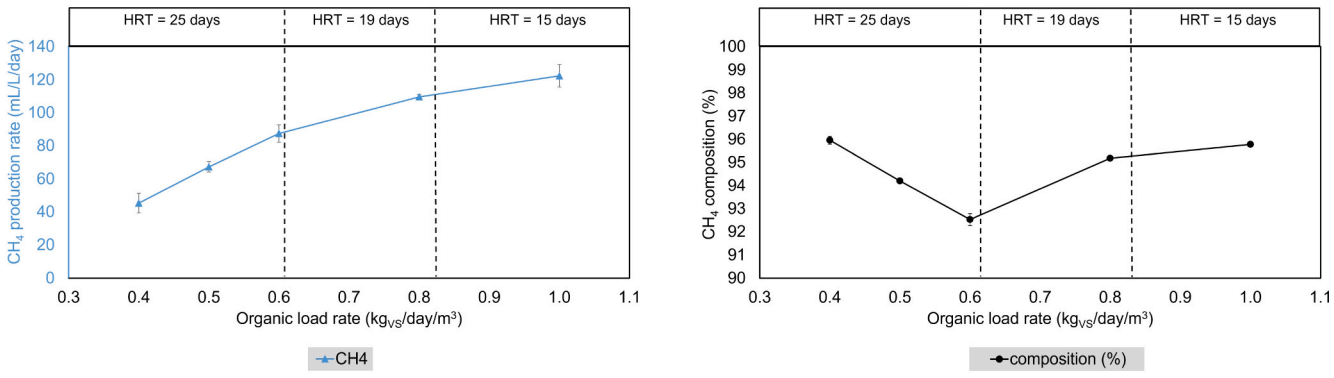

Fig. 1. Digestion of an alkaline sludge residue generated from the EPS extraction of AGS. Methane production rate (mL/L/day; y-axis left) and methane purity in the gas phase (%; y-axis right) versus OLR ($kg_{VS}/day/m^3$; x-axis).

experiment (Fig. 2). The pH values presented are the average values measured over 6 distinct days, after a complete HRT cycle for every OLR stage.

Although the influent fed had an average pH of 9.3 (Table 3), the operational pH for all OLR ranged between 8.6 and 8.8, indicating a pH drop within the reactor due to the microbial activity. First, the pH decreased linearly from 8.7 to 8.6 with increasing OLRs of 0.4; 0.5, and 0.6 $kg_{VS}/day/m^3$. Subsequently, the pH increased from 8.6 to 8.8 with increasing OLRs of 0.8 and 1 $kg_{VS}/day/m^3$.

This pH profile is a result of the increase in microbial CO_2 production and the decrease in HRT. In fact, an increase in methane production in AD, due to higher VS feeding or substrate conversion efficiency, is associated with an increase in CO_2 production. CO_2 is part of an acid-base system and an increase in CO_2 will lead to a decrease in pH. The rate of decrease of the pH is directly associated with the buffering capacity of the system (alkalinity) which remained constant at all stages (Table 3). On the other hand, the operational pH is affected by the pH of the influent, which in this case was around 9.3 (Table 3). By decreasing the HRT, the rate at which the influent replaces the reactor volume increases, which in turn increases the pH.

To elucidate the relationship between operational pH and biogas composition the geochemical modelling software PHREEQC was used (section 2.6). The goal of this model was to understand if pH and CH_4 purity variations are related, and if these variations could be fully justified by the chemical reactions, such as CO_2 production and NH_4 formation within the bioreactor. This model consisted of a closed system reactor where a gas and liquid phase are in equilibrium and it is fully described in section 2.6.

Modelled and observed experimental CH_4/CO_2 ratio in the gas phase are given in Fig. 3. The model is able to describe the general pattern observed experimentally for the CH_4 to CO_2 ratio as a function of pH. Both results fall within the same order of magnitude and the maximum ratio (~23) was observed around pH 8.6 for both the experimental and model results. However, the model and experimental results show an increase divergence for lower pHs (<8.6) by a factor of 1.5. For lower pHs, the CH_4/ CO_2 ratio for experimental results decreases more sharply in comparison to the modelled results.

3.4. Ammonia

Working at a higher pH leads to the speciation of ammonia towards free-ammonia (NH_3). NH_3 has been shown to inhibit anaerobic digestion, especially affecting the methanogenic community (Moerland et al., 2021). The NH_4 and NH_3 concentrations in relation to the OLR are given in Fig. 4.

Fig. 4 shows an increase from 28 ± 2 mM to 30.8 ± 1 mM in NH_4 concentrations for OLRs 0.4 to 0.6 kg_{VS}/day/m3. This is due to the increase of the substrate concentration in the influent, as the OLR was changed by increasing the initial VS concentration. For OLRs 0.8 and 1 kg_{VS}/day/m3, the NH_4 concentration increased slightly to around 40 mM. For NH_3 the opposite relation was observed. For OLRs 0.4; 0.5, and 0.6 $kg_{VS}/day/m^3$ the NH_3 concentration remained constant around 7 mM and for OLRs 0.8 and 1 $kg_{VS}/day/m^3$ the concentration increased to 9.6 ± 0.2 mM and to 13.6 ± 0.2 mM, respectively. This NH_3 profile directly relates to the operational pH (Fig. 2), as a higher pH leads to a higher NH_3 speciation over NH_4.

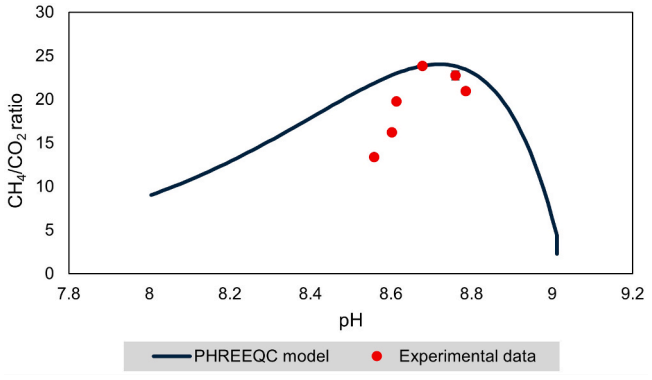

Fig. 3. The CH_4/CO_2 ratio in the gas phase according to the operational pH. The red dots (●) represent the experimental data observed. The black line (-) represents the chemical PHREEQC model results. The model is described in detail in section 2.6. (For interpretation of the references to colour in this figure legend, the reader is referred to the web version of this article.)

3.5. Microbial community

The bioreactor was sampled at the beginning and end of each OLR stage for DNA extraction to monitor the microbial community under different operational conditions. Fig. 5 shows the 16 s abundance for the top 10 bacteria at a taxonomy order level, and Fig. 6 shows the 16 s abundance for the top 10 archaea at a taxonomy genus level. Archaea is presented separately to provide a more focused look of changes observed in methanogens.

Fig. 5 shows a diversity of anaerobic fermentative bacteria at the class level. There is a significant presence of the class *Saccharimonadia* especially in the final stage of OLR 0.5 $kg_{VS}/day/m^3$. This class belongs to the Candidatus phylum *Patescibacteriota*, which is part of the Candidate Phyla Radiation (CPR). CPR mainly consists of uncultured, poorly understood anaerobic bacteria which are often parasitic or symbiotic and have a reduced genome and size (Castelle et al., 2018). This class has been mostly associated with monosaccharide and polysaccharide fermentation (Albertsen et al., 2013). Members of this group have been identified as one of the dominant bacterial classes in the sediments of Siberian soda lakes, the inoculum used in this study (Vavourakis et al., 2018). Additionally, it is possible to see a consistent presence of the class *Clostridia*. By looking at a deeper taxonomic level, most of this class belonged to the order *Peptostreptococcales-Tissierellales* which is associated with amino-acid fermentation (Ezaki, 2015). The class *Actinobacteria* is also found in all samples, however its relative abundance decreases for the higher OLRs. This class can be mainly found in soil and marine ecosystems and it is often associated with polysaccharide hydrolysis (Ranjani et al., 2016). In contrast, the relative abundance of the class *Bacteroidia* increases for higher OLRs. This class can be also linked to hemicellulose polysaccharide hydrolysis and dead biomass recycling. Lastly, a notable presence of the class *Dethiobacteria* was observed. Both characterized and uncultured members of this class are typically found in alkaline anaerobic environments, such as soda lakes and alkaline mineral springs. They are involved in autotrophic acetogenesis and the syntrophic oxidation of volatile fatty acids (VFA) (Sorokin & Merkel, 2022).

Fig. 6 gives a focused look into the archaeal community present in the reactor at the genus level. It shows an increase in dominance of the genus *Methanosaeta* until the OLR 0.6 $kg_{VS}/day/m^3$ and then a subsequent decrease in abundance. In Fig. 6, this genus includes the alkali-tolerant and alkaliphilic members that were recently reclassified to the genus *Methanocrinis* (Khomyakova et al., 2023). This genus is associated to alkaliphilic acetoclastic methanogens. Acetoclastic methanogens produce CH_4 and CO_2 through the breakdown of acetate. In parallel, the abundance of the genus *Methanocalculus* starts to increase from OLR 0.6 $kg_{VS}/day/m^3$ reaching dominance in the final samples. This genus includes mostly salt-tolerant hydrogenotrophic methanogens, from neutral salt habitats (Ollivier et al., 1998) to soda lakes (Sorokin et al., 2015; Zhilina & Zavarzin, 1994). Hydrogenotrophic methanogens produce CH_4 from CO_2 by using either H_2 or formate as an electron donor. In addition, the haloalkaliphilic *Methanocalculus* species have been shown to be the syntrophic H_2-consuming partners for the VFA-oxidizing syntrophic *Firmicutes* from soda lakes (Sorokin et al., 2015; Timmers et al., 2018). Fig. 6 shows a smaller presence of other genera of hydrogenotrophic methanogens such as *Methanobacterium,*

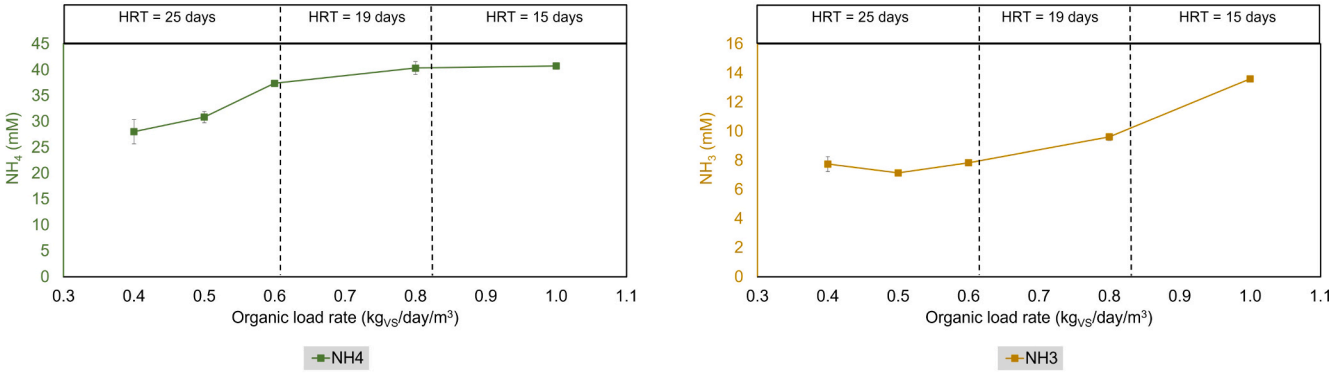

Fig. 4. NH_4 (left) and NH_3 (right) concentrations (mM) versus OLR ($kg_{VS}/day/m^3$; x-axis) from the digestion of a alkaline waste. The NH_4-NH_3 speciation was calculated according to the operational pH (Table 3) and the dissociation constant (pka) of 9.25 (Moerland et al., 2021).

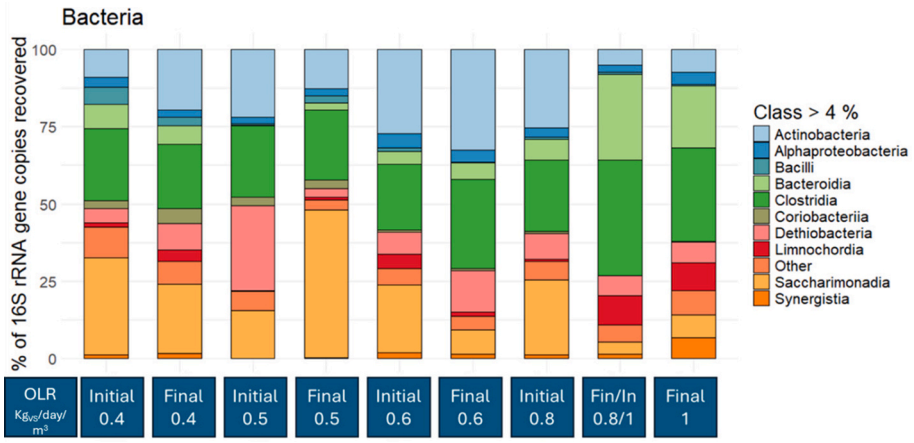

Fig. 5. Relative abundance of bacterial species for an initial and final sample to each OLR stage (0.4; 0.5; 0.6; 0.8; 1 $kg_{VS}/day/m^3$). The final sample for OLR 0.8 $kg_{VS}/day/m^3$ also represents the initial sample for 1 $kg_{VS}/day/m^3$. The results are presented at class level, for classes with an abundance higher than 4 %, classes with lower abundance are classified as other. Extraction and processing methods are described in section 2.5.

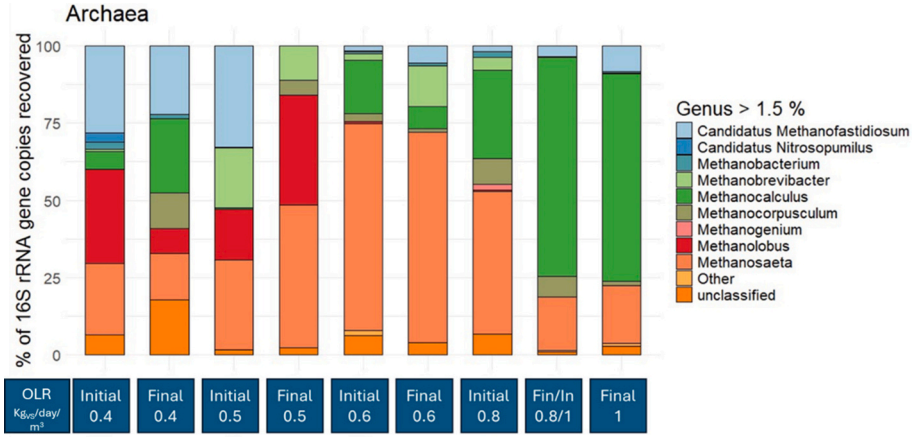

Fig. 6. Relative abundance of archaea species for an initial and final sample to each OLR stage (0.4; 0.5; 0.6; 0.8; 1 $kg_{VS}/day/m^3$). The final sample for OLR 0.8 $kg_{VS}/day/m^3$ also represents the initial sample for 1 $kg_{VS}/day/m^3$. The results are presented at genus level, for classes with an abundance higher than 1.5 %, genera with lower abundance are classified as other and genera that was not possible to classify is named unclassified. Extraction and processing methods are described in section 2.5.

Methanocorpusculum and Methanobrevibacter (Pasalari et al., 2021, Martinez-Romero et al., 2022; Dighe et al., 2004). Finally, salt-tolerant methylotrophic methanogens from the genus *Methanolobus* and methyl-reducing *Candidatus* Methanofastidiosum were also detected. The former is present in soda lakes and can ferment C_1-metyhyl compounds to methane and CO_2, while the latter is detected in marine habitats and is suggested to reduce methyl-sulfide to methane and H_2S using H_2 as the electron donor.

4. Discussion

4.1. Methane production and purity

This study demonstrated that AD under high-pH and high-alkalinity conditions for an alkaline waste with in-situ biogas upgrading is a possible and scalable process. The major bottleneck for in-situ biogas upgrading is considered to be the required high operational pH within the AD system and a methanogenic community that can handle these conditions (Khan et al., 2021). In the current work, this bottleneck was addressed by using a soda lake microbial community as an inoculum. Soda lakes are naturally occurring environments with high carbonate alkalinity levels and a high pH (9.5–11), in which a specialized and adapted microbial community is present (Schagerl & Renaut, 2016; Sorokin et al., 2014). In addition, the current study focused on a gradual increase of the OLR from 0.4 to 1 $kg_{VS}/day/m^3$, due to unestablished kinetics of the inoculum used and concerns over ammonia toxicity and potentially other inhibiting compounds. As a result, with an acclimatized soda lake community it was possible to reach a maximum specific methane production rate of 8.4 ± 0.5 $mL/day/g_{VSadded}$ with a corresponding methane purity in the gas phase of 95.8 ± 0.1 % for an OLR 1 $kg_{VS}/day/m^3$ (Table 4). Notably, at this OLR the VS conversion decreased by 8 % with a corresponding increase in the acetate concentration of the effluent. Acetate was only detected at the highest OLR stage suggesting that it was fully converted into CH_4 for the previous stages. This indicates, a transition from a hydrolysis-limited AD process to a methanogenesis-limited AD process at the last OLR stage (Ma et al., 2013). In addition, at this OLR stage the ammonium concentration remained the same per VS added (Fig. 4) indicating that hydrolysis remained constant between the last two stages.

Compared to the preliminary work on this process by Nolla-Ardèvol et al., (2015), the current study demonstrated a 75 % higher maximum methane specific production rate ($mL/day/g_{VSadded}$) and a higher methane gas content at an OLR of 1 $kg_{VS}/day/m^3$ (Table 4). Nolla-Ardèvol et al., (2015) performed alkaline methanation at a pH of 10 and at an alkalinity of 1.2–1.9 eq/L using microalga *Spirulina* as a substrate. In their work, the maximum specific methane production rate was 4.8 ± 1.0 $mL/day/g_{spir.added}$ for an OLR of 0.25 $kg_{VS}/day/m^3$ with corresponding 86 ± 5 % in methane content (Table 4). For an OLR of 1 $kg_{VS}/day/m^3$ the specific methane production rate was 2.0 ± 0.3 $mL/day/g_{VSadded}$ (Table 4). This decrease in production rate was hypothesized to be due to ammonia inhibition. The NH_3 concentration for the OLR of 1 $kg_{VS}/day/m^3$ was around 50 mM—3.5 times higher than the maximum concentration observed in the current work (13.6 ± 0.2 mM). The ammonia concentration was higher due to a combination of a higher operational pH (pH 10), which shifted the speciation towards NH_3 over NH_4, and the use of a protein-rich substrate (*Spirulina* biomass). This type of substrate has a low C/N ratio leading to higher nitrogen mineralization (Gonzalez-Fernandez et al., 2015). In fact, Samson & Leduy, (1983) showed that increasing the C/N from 4.2 to 6.2 by co-digesting *Spirulina* with sewage sludge enhanced CH_4 production. Alternatively, the higher methane specific production observed in the current study in comparison to Nolla-Ardèvol et al., (2015) work, could be related to microbial adaptation of the soda lake inoculum to the alkaline substrate used. As the soda lake inoculum used in the current study had a 200 day acclimatization period before the reactor operation started (section 2.2).

Table 4 compares the current results to the work of Val Del Río et al., (2014), where AD was performed at similar operational conditions using a relatively similar substrate at neutral pH and low alkalinity conditions. Their work used AGS and thermal-pre-treated AGS as a substrate. At a neutral pH for the same OLR of 1 $kg_{VS}/day/m^3$ a similar specific methane production rate (10.4 ± 3.0 mL $/day/g_{VSadded}$) and conversion in VS (32 %) was achieved for the neutral digestion conditions. However, at neutral conditions the thermal-pretreated AGS yielded a higher specific methane production rate (15.5 ± 3.0 $mL/day/g_{VSadded}$) and conversion in VS (47 %). For both cases the methane content in the gas phase was lower (62.4 ± 9.0 % and 64 ± 3.0, respectively), compared to one observed in the current work (95.8 ± 0.1 %). The lower specific methane production rate in the alkaline digester compared to the neutral results could be due to differences in substrates. The substrate used in the current work was the alkaline waste after EPS extraction from AGS through a thermo-alkaline process (Bahgat et al., 2023). The substrate for the alkaline fermentation comes without a significant fraction (ca. 25 %) of easily degradable biomass (Bahgat et al., 2023). This biomass is removed as biopolymer during the EPS extraction process and is primarily composed of proteins and sugars. Our proof-of-concept study indicates that anaerobic digestion (AD) at high pH and high alkalinity is a feasible process. In this approach, in-situ purification occurs, and the results show comparable specific methane production and conversion rates to those observed in neutral digestion, as shown in Table 4.

To fully understand the industrial impact of technology a further increase in OLR should be investigated, as anaerobic digesters for municipal sewage sludge are commonly operated at OLR of 2–5 $kg_{VS}/day/m^3$ (Uddin & Wright, 2023). For scale-up purposes, a balance between the microbial community's salt requirements and the feasibility of an industrial process should be further investigated, as the current salt load is impractical for industrial applications.

4.2. pH stability and its impact on gas composition

The operational pH slightly varied between 8.6 and 8.8 (Fig. 2). In order to understand if these variations could be fully related to CO_2 production by microbial activity, a chemical model was developed and compared with the experimental results (Fig. 3). Despite these pH changes, in-situ biogas purification occurred for all OLR stages studied, as the CH_4 purity remained above 90 % for all stages and above 95 % for the OLRs of 0.4, 0.8 and 1 $kg_{VS}/day/m^3$. This purification was done without any pH control and solely relied on the initial pH and alkalinity

Table 4
Comparison of anaerobic Digestion Process Parameters. Overview of Literature on high-pH and high-alkalinity anaerobic digestion and comparison with a neutral digestion process.

Study	pH	substrate	OLR (kg_{VS}/day/m^3)	HRT (day)	Specific CH_4 production rate (mL/day/$g_{VSadded}$)	CH_4 yield (mL/$g_{VSadded}$)	CH_4 (%)	CO_2 (%)	VS conversion (%)
This work	8.76 ±0.01	Alkaline pellet from EPS extraction from AGS	1	15	8.4 ± 0.5	126 ± 8	95.8 ± 0.1	4.2 ± 0.1	38 ± 1
(Nolla-Ardèvol et al., 2015)	10	microalga *Spirulina* biomass	0.25	15	4.8 ± 1.0	72 ± 12	86 ± 5	4 ± 3	11
			1	15	2.0 ± 0.3	30.7 ± 5	83 ± 9	14 ± 6	5
(Val Del Río et al., 2014)	7.4 ± 0.2	AGS	1	20	10.4 ± 3.0	208 ± 52	62.4 ± 9.0	25.9 ± 2.0	32
		Thermal pre-treated AGS	0.8–2.1	20	15.5 ± 3.0	309 ± 58	64 ± 3	25.9 ± 2.0	47

of the alkaline pellet diluted in the carbonate buffer (section 2.1). This demonstrates that alkaline fermentation can produce biomethane with a CO_2 content that can be directly injected into the gas grid without any ex-situ purification step, as CH_4 values rose above the 95 % standard for the final OLRs (Thrän et al., 2014). Skipping the ex-situ purification step is advantageous as these methods often are associated with high energy consumption and high operational costs (Khan et al., 2021).

Noorman et al., (1992) highlighted the importance and the complexity of modelling the bicarbonate/ carbonate speciation within alkaline systems, as microbial CO_2 production cannot be fully understood by the CO_2 present in the gas phase. Fig. 3 illustrates that the pH and gas concentration variations in the reactor can, to an extent, be modelled based on the chemical interactions (e.g. speciation) within this system. The model demonstrated a clear relationship between reactor pH changes and microbial CO_2 production (Fig. 3). Both experimental and modelled results fell within the same order of magnitude with both reaching a maximum in CH_4/ CO_2 ratio in the gas phase around pH 8.6. At pH 8.6 the relative speciation of the dissolved CO_2 $(CO_2(aq))$ in equilibrium with carbonate (CO_3^{-2}) and bicarbonate (HCO_3^-) drops to zero, possibly creating this shift in the ratio (Middelburg et al., 2020).

However, the model results diverge from the experimental results for lower pH ranges, as a sharper decrease in the CH_4/ CO_2 ratio is observed for the experimental results. This suggests a higher CO_2 outgassing than predicted or a significant change in the CH_4 and CO_2 stoichiometries in the product reaction, since the model is based on this reaction (formula 3). A change in the stoichiometries of the product reaction would also lead to a deviation between the theoretical and experimental specific methane production rate (Table 3), which was not observed. Suggesting the assumed product reaction is valid and leading to the conclusion that experimentally there is higher CO_2 outgassing than what is predicted in the model for pHs below 8.6. In addition, the model overestimated the average alkalinity, the average alkalinity in the bioreactor was 0.5 ± 0.02 eq/L, whilst the average predicted alkalinity in the model was 0.57 ± 0.01 eq/L.

A constraint of the model is the assumption that organic matter does not play a role in the chemical interactions within the bioreactor. The model did not take into account both the VFAs loaded and released throughout the anaerobic digestion, which could have played a role in pH variations. VFAs have also been shown to create a buffering system with ammonia which was not taken into account in the model (Wang et al., 2013). Additionally, the model also did not consider the potential absorption of ammonia and phosphate on suspended organic solids, which in turn effects the alkalinity (de Visscher et al., 2002; Sui & Thompson, 2000). Finally, the potential salts present in the alkaline residue used were not considered, only the salts in the carbonate buffer were considered. This may have resulted in key chemical interaction such as precipitation being overlooked. To further improve this model a full characterization of the alkaline substrate used should be done and suspended organic fraction should be considered. Another constrain in the model is that it fully relies on the database used and the respective dissociation constants. For pure chemical systems, It has been shown that the theoretical dissociation constants for the bicarbonate/carbonate system slightly diverge from the expected for high-salinity environments (Millero et al., 2006).

In conclusion, despite pH variations, in-situ biogas upgrading occurred at all OLR stages studied. Changes in the methane purity can only be partially explained by microbial CO_2 production through a geochemical model. This highlights the complex relationship between microbial activity and the chemical processes within this system. For future applications, these dynamics and how they affect methane purity should be further studied and validated trough experimental data. The model should be expanded to include the impact of organic matter.

4.3. Ammonia

Several studies have shown that free ammonia nitrogen (NH_3) can inhibit methanogenesis during anaerobic digestion. It is generally established that anaerobic digestion at neutral conditions is inhibited by concentrations of total ammonia nitrogen (TAN) between 143–275 mM (Moerland et al., 2021). For mesophilic conditions and a pH of 7.5 this corresponds to free-ammonia (NH_3) concentrations between 3–6 mM. However, this range is highly dependent on the substrate used and the adaption of the microbial community to it. In fact, for the digestion of municipal solid waste at mesophilic conditions a 50 % inhibition was observed for a NH_3 concentration of 12 mM (Benabdallah El Hadj et al., 2009).

A maximum of 13.6 ± 0.2 mM of NH_3 was reached in the present study with the highest OLR of 1 $kg_{VS}/day/m^3$ (Fig. 4). At this concentration a significant methane production was observed, indicating that no or very limited inhibition occurred. However, the rate at which CH_4 production increased slowed down for the last OLR increase (Fig. 1). This could be related to the ammonia concentration or to other factor such as kinetic limitations. Nolla-Ardèvol et al., (2015) used a similar soda lake inoculum and a 50 % ammonia inhibition was only observed for NH_3 concentrations above 50 mM. These observations suggest that the alkaliphilic methanogens from soda lakes have a higher resistance to NH_3 concentrations than typical neutrophilic methanogens found in anaerobic digesters. It is hypothesized that ammonia inhibition is caused by the passive diffusion of NH_3 through the cell membrane (Kayhanian, 1999).

Alkaliphilic bacteria and archaea have been shown to have microbial adaptations to avoid proton leakage. The microbial adaptions range from bioenergetic adaptations, such as the use of Na^+-dependant ATPases (Angelini et al., 2012); to osmoprotectant adaptations, such as the use salt-in strategy (Mesbah & Wiegel, 2011); and to membrane adaptations such as the incorporation of squalene (Siliakus et al., 2017) or the incorporation of specialized lipids (de Jong, 2024). In fact, It has been shown that archaea belonging to the *Methanocrinis* genus found in the current study synthetized ectoine as a osmoprotectant at high pH conditions (Khomyakova et al., 2023). These adaptations could lead to a lower NH_3 diffusion and in turn to a higher resistance towards NH_3. If the OLR would be further increased to 2 $kg_{VS}/day/m^3$, considering a constant pH, the NH_3 concentration would be around 30 mM, which would still be below the concentrations observed by Nolla-Ardèvol et al., (2015)) as inhibitory. We thus hypothesize that in an industrial competitive feeding regime NH_4 should not be a limiting factor. In addition, other strategies such as ammonia stripping have been proposed to mitigate ammonia inhibition and improve AD efficiency which could be applied in tandem with this technology (Yellezuome et al., 2022). The effects of ammonia on alkaliphilic methanogens should be further studied as no limitation was observed in the studied conditions. This suggests that alkaliphilic methanogens have a higher resistance to NH_3 concentrations.

4.4. Microbial community

Fig. 5 and Fig. 6 illustrate the changes in the microbial community for bacteria and archaea, respectively. The bacterial community composition remained relatively stable throughout the reactor operation. While shifts in dominance were observed, the overall taxonomic classes present remained largely unchanged. Most of the observed bacterial taxonomic classes were linked to anaerobic fermentation of polymers and monomers, with some also associated with salt tolerance. This reflects the complexity of the alkaline substrate used. In fact, it was possible to see a significant abundance of classes associated with polysaccharide and monosaccharide fermentation (*Saccharimonadia, Bacteroidia*), cellulose fermentation (*Actionobacteria*) and amino-acid fermentation (order: *Peptostreptococcales-Tissierellales*). The current study also showed the class *Saccharimonadia*, a member of the Candidate

Phyla Radiation, as a dominant bacterial group in a haloalkaline culture. This class has been found in the metagenome of soda lake anaerobic sediments (Vavourakis et al., 2018). Recently, this class has been shown to be associated with acetoclastic methanogenic archaea, such as the class *Methanosaeta* found in this study, in a bioreactor at a neutral pH conditions (Kuroda et al., 2022).

In contrast, the archaeal community changed throughout the reactor run. Genera associated with methanogenesis and salt-tolerance were dominant overall. However, there was a shift from acetate-dependent methanogenesis (acetoclastic) to hydrogen-dependent methanogenesis (hydrogenotrophic). The genus *Methanosaeta*, associated with acetoclastic methanogenesis (Khomyakova et al., 2023), increased in abundance until the 0.6 $kg_{VS}/day/m^3$ final sample and subsequently decreased in abundance. In parallel, the genus *Methanocalculus*, associated with hydrogenotrophic methanogenesis (Ollivier et al., 1998), increased in abundance from the 0.6 $kg_{VS}/day/m^3$ final sample, reaching dominance at the OLR of 1 $kg_{VS}/day/m^3$. This shift could have caused by the variations in pH as the 0.6 $kg_{VS}/day/m^3$ OLR represents a shift point from a pH decrease profile to a pH increase profile (Fig. 2). Throughout literature, it is reported that the acetoclastic route is inhibited at higher pHs and the hydrogenotrophic route becomes dominant (Zhilina & Zavarzin, 1994; Wormald et al., 2020). This shift is reflected in our findings, the decrease in pH from OLR 0.4 to 0.6 $kg_{VS}/day/m^3$ is associated with an increase in the dominance of acetate-dependent methanogenesis, while the subsequent increase in pH from OLR 0.6 to 1 $kg_{VS}/day/m^3$ correlates with a rise in hydrogen-dependent methanogenesis. Knowing the pH range at which this acetoclastic to hydrogenotrophic shift occurs, is beneficial for future reactor design as it is possible to select the preferred methanogenesis metabolic pathway.

5. Conclusion

This study demonstrated that anaerobic digestion can be effectively conducted under high-pH and high-alkalinity conditions using a complex alkaline waste substrate in a continuous mode. It served as a proof of concept for this technology, providing a foundation for full-scale processes. It demonstrated scalability by increasing organic loading rates without encountering ammonium inhibition. The maximum specific methane production obtained was 8.4 ± 0.5 mL//day/$g_{VSadded}$ for an HRT of 15 days and a OLR of 1 $kg_{VS}/day/m^3$. The maximum conversion observed was 48.1 ± 1.1 % in VS. Moreover, the methane gas purity consistently exceeded 90 %, peaking at 96.0 ± 0.2 %, indicating a robust in-situ biogas purification. These findings matched with the specific methane production rates seen in neutral pH digestion, and also position alkaline anaerobic digestion as a promising, industrially viable solution for managing alkaline waste. It facilitates both effective waste treatment and high-quality methane production.

CRediT authorship contribution statement

Beatriz C. Diniz: Writing – original draft, Software, Project administration, Methodology, Investigation, Formal analysis, Data curation. **Philipp Wilfert:** Writing – review & editing, Validation, Supervision, Resources, Project administration, Conceptualization. **Dimitry Y. Sorokin:** Writing – review & editing, Validation, Supervision, Conceptualization. **Mark C.M. van Loosdrecht:** Writing – review & editing, Supervision, Resources, Project administration, Funding acquisition, Conceptualization.

Declaration of competing interest

The authors declare that they have no known competing financial interests or personal relationships that could have appeared to influence the work reported in this paper.

Acknowledgements

The authors would like to thank and acknowledge Valarie Sels, Lena Depaz and Gerben Stout on their initial work done on high-pH and high-alkalinity digestion. Within this initial work a special thanks goes to Ramon Zwaan for providing the initial inoculum used in this study.We would also like to thank all the technical support provided by Dirk Geerts, Dita Heikens, Ben Abbas, Zita van der Krogt and Kevin de Carlo. In addition, we thank Nouran Bahgat for executing the elemental analysis shown in this work. This research was funded by the SIAM Gravitation Grant 024.002.002 and by the Spinoza Award to Mark van Loosdrecht, both from the Netherlands Organization for Scientific Research (NWO).

Appendix A. Supplementary data

Supplementary data to this article can be found online at https://doi.org/10.1016/j.biortech.2025.132505.

Data availability

Data will be made available on request.

References

Albertsen, M., Hugenholtz, P., Skarshewski, A., Nielsen, K.L., Tyson, G.W., Nielsen, P.H., 2013. Genome sequences of rare, uncultured bacteria obtained by differential coverage binning of multiple metagenomes. Nat. Biotechnol. 31 (6), 533–538. https://doi.org/10.1038/nbt.2579.

Angelini, R., Corral, P., Lopalco, P., Ventosa, A., Corcelli, A., 2012. Novel ether lipid cardiolipins in archaeal membranes of extreme haloalkaliphiles. Biochim. Biophys. Acta Biomembr. 1818 (5), 1365–1373. https://doi.org/10.1016/j.bbamem.2012.02.014.

APHA, 2017. Standard Methods for the Examination of Water and Wastewater, 23rd ed.

Awe, O.W., Zhao, Y., Nzihou, A., Minh, D.P., Lyczko, N., 2017. A review of biogas utilisation, purification and upgrading technologies. Waste Biomass Valoriz. 8 (2), 267–283. https://doi.org/10.1007/s12649-016-9826-4.

Bahgat, N.T., Wilfert, P., Korving, L., Van Loosdrecht, M., 2023. Integrated resource recovery from aerobic granular sludge plants. Water Res. 234, 119819. https://doi.org/10.1016/j.watres.2023.119819.

Benabdallah El Hadj, T., Astals, S., Galí, A., Mace, S., Mata-Álvarez, J., 2009. Ammonia influence in anaerobic digestion of OFMSW. Water Sci. Technol. 59 (6), 1153–1158. https://doi.org/10.2166/wst.2009.100.

Boarino, A., Demichelis, F., Vindrola, D., Robotti, E., Marengo, E., Martin, M., Deorsola, F., Padoan, E., Celi, L., 2024. Bio-physical pre-treatments in anaerobic digestion of organic fraction of municipal solid waste to optimize biogas production and digestate quality for agricultural use. Waste Manag. 189, 114–126. https://doi.org/10.1016/j.wasman.2024.08.023.

Bokulich, N.A., Subramanian, S., Faith, J.J., Gevers, D., Gordon, J.I., Knight, R., Mills, D. A., Caporaso, J.G., 2013. Quality-filtering vastly improves diversity estimates from Illumina amplicon sequencing. Nat. Methods 10 (1), 57–59. https://doi.org/10.1038/nmeth.2276.

Boyd, C.E., 2020. Carbon dioxide, pH, and alkalinity. In: Boyd, C.E. (Ed.), Water Quality. Springer International Publishing, pp. 177–203 doi: 10.1007/978-3-030-23335-8_9.

Cai, M., Wilkins, D., Chen, J., Ng, S.-K., Lu, H., Jia, Y., Lee, P.K.H., 2016. Metagenomic reconstruction of key anaerobic digestion pathways in municipal sludge and industrial wastewater biogas-producing systems. Front. Microbiol. 7. https://doi.org/10.3389/fmicb.2016.00778.

Callahan, B.J., McMurdie, P.J., Rosen, M.J., Han, A.W., Johnson, A.J.A., Holmes, S.P., 2016. DADA2: High-resolution sample inference from Illumina amplicon data. Nat. Methods 13 (7), 581–583. https://doi.org/10.1038/nmeth.3869.

Castelle, C.J., Brown, C.T., Anantharaman, K., Probst, A.J., Huang, R.H., Banfield, J.F., 2018. Biosynthetic capacity, metabolic variety and unusual biology in the CPR and DPANN radiations. Nat. Rev. Microbiol. 16 (10), 629–645. https://doi.org/10.1038/s41579-018-0076-2.

Chen, X.Y., Vinh-Thang, H., Ramirez, A.A., Rodrigue, D., Kaliaguine, S., 2015. Membrane gas separation technologies for biogas upgrading. RSC Adv. 5 (31), 24399–24448. https://doi.org/10.1039/C5RA00666J.

Daelman, M.R.J., Sorokin, D., Kruse, O., Van Loosdrecht, M.C.M., Strous, M., 2016. Haloalkaline Bioconversions for Methane Production from Microalgae Grown on Sunlight. Trends Biotechnol. 34 (6), 450–457. https://doi.org/10.1016/j.tibtech.2016.02.008.

de Jong, S. I. (2024). *Alkaliphilic Life: Adaptation strategies by Caldalkalibacillus thermarum* [Delft University of Technology]. doi: 10.4233/UUID:EF90D088-F7AC-4767-A926-3B4BAC9497E9.

de Visscher, A., Harper, L.A., Westerman, P.W., Liang, Z., Arogo, J., Sharpe, R.R., van Cleemput, O., 2002. Ammonia emissions from anaerobic swine lagoons: model

development. J. Appl. Meteorol. 41 (4), 426–433. https://doi.org/10.1175/1520-0450(2002)041<0426:AEFASL>2.0.CO;2.
Dighe, A.S., Jangid, K., González, J.M., Pidiyar, V.J., Patole, M.S., Ranade, D.R., Shouche, Y.S., 2004. Comparison of 16S rRNA gene sequences of genus Methanobrevibacter. BMC Microbiol. 4 (1), 20. https://doi.org/10.1186/1471-2180-4-20.
Dunnivant, F.M., 2004. Environmental Laboratory Exercises For Instrumental Analysis and Environmental Chemistry. Wiley-Interscience.
Ezaki, T., 2015. Peptostreptococcus. In: Whitman, W.B. (Ed.), Bergey's Manual of Systematics of Archaea and Bacteria, 1st ed. Wiley, pp. 1–4. doi: 10.1002/9781118960608.gbm00668.
Gonzalez-Fernandez, C., Sialve, B., Molinuevo-Salces, B., 2015. Anaerobic digestion of microalgal biomass: Challenges, opportunities and research needs. Bioresour. Technol. 198, 896–906. https://doi.org/10.1016/j.biortech.2015.09.095.
Gujer, W., Zehnder, A.J.B., 1983. Conversion Processes in Anaerobic Digestion. Water Sci. Technol. 15 (8–9), 127–167. https://doi.org/10.2166/wst.1983.0164.
Karthikeyan, P.K., Bandulasena, H.C.H., Radu, T., 2024. A comparative analysis of pre-treatment technologies for enhanced biogas production from anaerobic digestion of lignocellulosic waste. Ind. Crop. Prod. 215, 118591. https://doi.org/10.1016/j.indcrop.2024.118591.
Kayhanian, M., 1999. Ammonia inhibition in high-solids biogasification: an overview and practical solutions. Environ. Technol. 20 (4), 355–365. https://doi.org/10.1080/09593332008616828.
Khan, M.U., Lee, J.T.E., Bashir, M.A., Dissanayake, P.D., Ok, Y.S., Tong, Y.W., Shariati, M.A., Wu, S., Ahring, B.K., 2021. Current status of biogas upgrading for direct biomethane use: A review. Renew. Sustain. Energy Rev. 149, 111343. https://doi.org/10.1016/j.rser.2021.111343.
Khomyakova, M.A., Merkel, A.Y., Slobodkin, A.I., Sorokin, D.Y., 2023. Phenotypic and genomic characterization of the first alkaliphilic aceticlastic methanogens and proposal of a novel genus Methanocrinis gen.nov. Within the family Methanotrichaceae. Front. Microbiol. 14, 1233691. https://doi.org/10.3389/fmicb.2023.1233691.
Kim, J.S., Lee, Y.Y., Kim, T.H., 2016. A review on alkaline pretreatment technology for bioconversion of lignocellulosic biomass. Bioresour. Technol. 199, 42–48. https://doi.org/10.1016/j.biortech.2015.08.085.
Kleerebezem, R., 2014. Biochemical Conversion: Anaerobic Digestion. In: De Jong, W., Van Ommen, J.R. (Eds.), Biomass as a Sustainable Energy Source for the Future, 1st ed. Wiley, pp. 441–468. doi: 10.1002/9781118916643.ch14.
Kuroda, K., Yamamoto, K., Nakai, R., Hirakata, Y., Kubota, K., Nobu, M.K., Narihiro, T., 2022. Symbiosis between *Candidatus* patescibacteria and archaea discovered in wastewater-treating bioreactors. MBio 13 (5), e01711–e01722. https://doi.org/10.1128/mbio.01711-22.
Labatut, R.A., Pronto, J.L., 2018. Sustainable waste-to-energy technologies: anaerobic digestion. In: Sustainable Food Waste-to-Energy Systems. Elsevier, pp. 47–67. https://doi.org/10.1016/B978-0-12-811157-4.00004-8.
Lombardi, L., Francini, G., 2020. Techno-economic and environmental assessment of the main biogas upgrading technologies. Renew. Energy 156, 440–458. https://doi.org/10.1016/j.renene.2020.04.083.
Lora Grando, R., De Souza Antune, A.M., Da Fonseca, F.V., Sánchez, A., Barrena, R., Font, X., 2017. Technology overview of biogas production in anaerobic digestion plants: A European evaluation of research and development. Renew. Sustain. Energy Rev. 80, 44–53. https://doi.org/10.1016/j.rser.2017.05.079.
Ma, J., Frear, C., Wang, Z., Yu, L., Zhao, Q., Li, X., Chen, S., 2013. A simple methodology for rate-limiting step determination for anaerobic digestion of complex substrates and effect of microbial community ratio. Bioresour. Technol. 134, 391–395. https://doi.org/10.1016/j.biortech.2013.02.014.
Martinez-Romero, J., Falcón, L.I., Aguirre-Noyola, J.L., Rosenblueth, M., Martinez-Romero, E., 2022. Microbial symbioses. Reference Module in Life Sciences. Elsevier, 10.1016/B978-0-12-822563-9.00038-X.
Mesbah, N.M., Wiegel, J., 2011. The Na+-translocating F1FO-ATPase from the halophilic, alkalithermophile Natranaerobius thermophilus. Biochim. Biophys. Acta (BBA) – Bioenerget. 1807 (9), 1133–1142. https://doi.org/10.1016/j.bbabio.2011.05.001.
Middelburg, J.J., Soetaert, K., Hagens, M., 2020. Ocean Alkalinity, Buffering and Biogeochemical Processes. Rev. Geophys. 58 (3), e2019RG000681. https://doi.org/10.1029/2019RG000681.
Millero, F.J., Graham, T.B., Huang, F., Bustos-Serrano, H., Pierrot, D., 2006. Dissociation constants of carbonic acid in seawater as a function of salinity and temperature. Mar. Chem. 100 (1–2), 80–94. https://doi.org/10.1016/j.marchem.2005.12.001.
Moerland, M.J., Bruning, H., Buisman, C.J.N., Van Eekert, M.H.A., 2021. Advanced modelling to determine free ammonia concentrations during (hyper-)thermophilic anaerobic digestion in high strength wastewaters. J. Environ. Chem. Eng. 9 (6), 106724. https://doi.org/10.1016/j.jece.2021.106724.
Nolla-Ardèvol, V., Strous, M., Tegetmeyer, H.E., 2015. Anaerobic digestion of the microalga Spirulina at extreme alkaline conditions: Biogas production, metagenome, and metatranscriptome. Front. Microbiol. 6. https://doi.org/10.3389/fmicb.2015.00597.
Noorman, H.J., Luijkx, G.C.A., Luyben, K.C.A.M., Heijnen, J.J., 1992. Modeling and experimental validation of carbon dioxide evolution in alkalophilic cultures. Biotechnol. Bioeng. 39 (11), 1069–1079. https://doi.org/10.1002/bit.260391102.
Ollivier, B., Fardeau, M.-L., Cayol, J.-L., Magot, M., Patel, B.K.C., Prensier, G., Garcia, J.-L., 1998. Methanocalculus halotolerans gen. Nov., sp. Nov., isolated from an oil-producing well. Int. J. Syst. Bacteriol. 48 (3), 821–828. https://doi.org/10.1099/00207713-48-3-821.
Oren, A., 1999. Bioenergetic aspects of halophilism. Microbiol. Mol. Biol. Rev. 63 (2), 334–348. https://doi.org/10.1128/MMBR.63.2.334-348.1999.
Pasalari, H., Gholami, M., Rezaee, A., Esrafili, A., Farzadkia, M., 2021. Perspectives on microbial community in anaerobic digestion with emphasis on environmental parameters: A systematic review. Chemosphere 270, 128618. https://doi.org/10.1016/j.chemosphere.2020.128618.
McMurdie, P.J., S.h., 2017. *Phyloseq* [Computer software]. Bioconductor. https://doi.org/10.18129/B9.BIOC.PHYLOSEQ.
Pfennig, N., Lippert, K.D., 1966. Uber das Vitamin B12-Bedrfnis phototropher Schwefelbakterien. Archiv Fur Mikrobiologie 55 (3), 245–256. https://doi.org/10.1007/BF00410246.
Ranjani, A., Dhanasekaran, D., Gopinath, P.M., 2016. An introduction to actinobacteria. In: Dhanasekaran, D., Jiang, Y. (Eds.), Actinobacteria—Basics and Biotechnological Applications. InTech doi: 10.5772/62329.
Rincón-Pérez, J., Celis, L.B., Morales, M., Alatriste-Mondragón, F., Tapia-Rodríguez, A., Razo-Flores, E., 2021. Improvement of methane production at alkaline and neutral pH from anaerobic co-digestion of microalgal biomass and cheese whey. Biochem. Eng. J. 169, 107972. https://doi.org/10.1016/j.bej.2021.107972.
Robeson, M.S., O'Rourke, D.R., Kaehler, B.D., Ziemski, M., Dillon, M.R., Foster, J.T., Bokulich, N.A., 2020. *RESCRIPt:* Reproducible sequence taxonomy reference database management for the masses [Preprint]. Bioinformatics. https://doi.org/10.1101/2020.10.05.326504.
Romero-Güiza, M.S., Wahid, R., Hernández, V., Møller, H., Fernández, B., 2017. Improvement of wheat straw anaerobic digestion through alkali pre-treatment: Carbohydrates bioavailability evaluation and economic feasibility. Sci. Total Environ. 595, 651–659. https://doi.org/10.1016/j.scitotenv.2017.04.006.
Samson, R., Leduy, A., 1983. Improved performance of anaerobic digestion ofSpirulinamaxima algal biomass by addition of carbon-rich wastes. Biotechnol. Lett 5, 677–682.
Schagerl, M., Renaut, R.W., 2016. Dipping into the Soda Lakes of East Africa. In: Schagerl, M. (Ed.), Soda Lakes of East Africa. Springer International Publishing, pp. 3–24. https://doi.org/10.1007/978-3-319-28622-8_1.
Siliakus, M.F., Van Der Oost, J., Kengen, S.W.M., 2017. Adaptations of archaeal and bacterial membranes to variations in temperature, pH and pressure. Extremophiles 21 (4), 651–670. https://doi.org/10.1007/s00792-017-0939-x.
Sorokin, D.Y., Abbas, B., Geleijnse, M., Pimenov, N.V., Sukhacheva, M.V., Van Loosdrecht, M.C.M., 2015. Methanogenesis at extremely haloalkaline conditions in the soda lakes of Kulunda Steppe (Altai, Russia). FEMS Microbiol. Ecol. 91 (4). https://doi.org/10.1093/femsec/fiv016.
Sorokin, D.Y., Berben, T., Melton, E.D., Overmars, L., Vavourakis, C.D., Muyzer, G., 2014. Microbial diversity and biogeochemical cycling in soda lakes. Extremophiles 18 (5), 791–809. https://doi.org/10.1007/s00792-014-0670-9.
Sorokin, D.Y., Merkel, A.Y., 2022. Dethiobacteria class. Nov. In: Whitman, W.B. (Ed.), Bergey's Manual of Systematics of Archaea and Bacteria, 1st ed. Wiley, pp. 1–3. doi: 10.1002/9781118960608.cbm00089.
Sui, Y., Thompson, M.L., 2000. Phosphorus sorption, desorption, and buffering capacity in a biosolids-amended mollisol. Soil Sci. Soc. Am. J. 64 (1), 164–169. https://doi.org/10.2136/sssaj2000.641164x.
Thrän, D., Billig, E., Persson, T., Svensson, M., Daniel-Gromke, J., Ponitka, J., Seiffert, M., with International Energy Agency & International Energy Agency, 2014. Biomethane: Status and Factors Affecting Market Development and Trade: a Joint Study. IEA Bioenergy.
Timmers, P.H.A., Vavourakis, C.D., Kleerebezem, R., Damsté, J.S.S., Muyzer, G., Stams, A.J.M., Sorokin, D.Y., Plugge, C.M., 2018. Metabolism and occurrence of methanogenic and sulfate-reducing syntrophic acetate oxidizing communities in haloalkaline environments. Front. Microbiol. 9, 3039. https://doi.org/10.3389/fmicb.2018.03039.
Toutian, V., Barjenbruch, M., Loderer, C., Remy, C., 2021. Impact of process parameters of thermal alkaline pretreatment on biogas yield and dewaterability of waste activated sludge. Water Res. 202, 117465. https://doi.org/10.1016/j.watres.2021.117465.
Uddin, M.M., Wright, M.M., 2023. Anaerobic digestion fundamentals, challenges, and technological advances. Phys. Sci. Rev. 8 (9), 2819–2837. https://doi.org/10.1515/psr-2021-0068.
Val Del Río, Á., Palmeiro-Sanchez, T., Figueroa, M., Mosquera-Corral, A., Campos, J.L., Méndez, R., 2014. Anaerobic digestion of aerobic granular biomass: Effects of thermal pre-treatment and addition of primary sludge. J. Chem. Technol. Biotechnol. 89 (5), 690–697. https://doi.org/10.1002/jctb.4171.
Vavourakis, C.D., Andrei, A.-S., Mehrshad, M., Ghai, R., Sorokin, D.Y., Muyzer, G., 2018. A metagenomics roadmap to the uncultured genome diversity in hypersaline soda lake sediments. Microbiome 6 (1), 168. https://doi.org/10.1186/s40168-018-0548-7.
Wang, Q., Peng, L., Su, H., 2013. The effect of a buffer function on the semi-continuous anaerobic digestion. Bioresour. Technol. 139, 43–49. https://doi.org/10.1016/j.biortech.2013.04.006.
Weiland, P., 2010. Biogas production: Current state and perspectives. Appl. Microbiol. Biotechnol. 85 (4), 849–860. https://doi.org/10.1007/s00253-009-2246-7.
Wormald, R.M., Rout, S.P., Mayes, W., Gomes, H., Humphreys, P.N., 2020. Hydrogenotrophic Methanogenesis Under Alkaline Conditions. Front. Microbiol. 11, 614227. https://doi.org/10.3389/fmicb.2020.614227.
Yellezuome, D., Zhu, X., Wang, Z., Liu, R., 2022. Mitigation of ammonia inhibition in anaerobic digestion of nitrogen-rich substrates for biogas production by ammonia stripping: A review. Renew. Sustain. Energy Rev. 157, 112043. https://doi.org/10.1016/j.rser.2021.112043.
Zhilina, T.N., Zavarzin, G.A., 1994. Alkaliphilic anaerobic community at pH 10. Curr. Microbiol. 29 (2), 109–112. https://doi.org/10.1007/BF01575757.